Selective imaging of internalized proteopathic α-synuclein seeds in primary neurons reveals mechanistic insight into transmission of synucleinopathies

Received for publication, February 7, 2017, and in revised form, June 11, 2017 Published, Papers in Press, June 13, 2017, DOI 10.1074/jbc.M117.780296

Richard J. Karpowicz, Jr.[‡], Conor M. Haney[§1], Tiberiu S. Mihaila[§], Raizel M. Sandler[‡], E. James Petersson[§], and Virginia M.-Y. Lee[‡2]

From the [‡]Center for Neurodegenerative Disease Research, Department of Pathology and Laboratory Medicine, Perelman School of Medicine, and the [§]Department of Chemistry, University of Pennsylvania, Philadelphia, Pennsylvania 19104

Edited by Paul E. Fraser

Direct cell-to-cell transmission of proteopathic α-synuclein (α-syn) aggregates is thought to underlie the progression of neurodegenerative synucleinopathies. However, the specific intracellular processes governing this transmission remain unclear because currently available model systems are limited. For example, in cell culture models of α-syn–seeded aggregation, it is difficult to discern intracellular from extracellular exogenously applied α-syn seed species. Herein, we employed fluorescently labeled α-syn preformed fibrils (pffs) in conjunction with the membrane-impermeable fluorescence quencher trypan blue to selectively image internalized α-syn seeds in cultured primary neurons and to quantitatively characterize the concentration dependence, time course, and inhibition of pff uptake. To study the long-term fates of exogenous α-syn pffs in neurons, we developed a pff species labeled at amino acid residue 114 with the environmentally insensitive fluorophore BODIPY or the pH-sensitive dye pHrodo red. We found that pffs are rapidly trafficked along the endolysosomal pathway, where most of the material remains for days. We also found that brief pharmacological perturbation of lysosomes shortly after the pff treatment causes aberrations in intracellular processing of pff seeds concomitant with an increased rate of inclusion formation via recruitment of endogenous α-syn to a relatively small number of exogenous seeds. Our results validate a quantitative assay for pff uptake in primary neurons, implicate lysosomal processing as the major fate of internalized proteopathic seeds, and suggest lysosomal integrity as a significant rate-determining step in the transmission of α-syn pathology. Further, lysosomal processing of transmitted seeds may represent a new therapeutic target to combat the spread of synucleinopathies.

Mounting evidence implicates direct cell-to-cell transmission of misfolded amyloidogenic protein species as a central component underlying the spatiotemporal progression of pathophysiology in numerous proteinopathies (1, 2). In synucleinopathies, including Parkinson's disease, Parkinson's disease with dementia, dementia with Lewy bodies, and multiple system atrophy, the amyloidogenic protein α-synuclein (α-syn)[3] aggregates into Lewy bodies, Lewy neurites, and glial cytoplasmic inclusions (3, 4). These intracellular proteinaceous inclusions have been widely recapitulated in a number of *in vivo* and cell-based model systems via introduction of pathological, insoluble α-syn species from either brain extracts of diseased postmortem tissue or preformed fibrils of recombinant origin (5–10). Despite strong evidence gleaned from these models implicating a causal relationship between exposure of neurons to insoluble α-syn aggregates and the subsequent development of inclusions bearing pathological hallmarks of synucleinopathies, the specific processes underlying cell-to-cell transmission of proteopathic seeds and resulting intracellular events leading to the development of pathological aggregates remain poorly understood. Whereas recent advances using flow cytometry or microfluidic culture chambers have been employed to study internalization and intracellular trafficking of amyloidogenic species, respectively, there exists a dearth of quantitative methods capable of unambiguous and spatially resolved discernment of intracellular from extracellular misfolded proteopathic species in a primary neuronal culture (11–15). As such, the study of the uptake and intracellular processing of proteopathic α-syn seeds, as well as their subsequent interaction with endogenous α-syn in the seeding of intracellular aggregates, has been impeded.

To overcome these limitations and to quantitatively characterize α-syn uptake and processing in cultured primary neurons, we adapted well-precedented fluorescence quenching techniques to the study of fluorophore-labeled α-syn preformed fibril (pff) uptake by primary neurons. Trypan blue is

This work was supported by National Institutes of Health Grants NS053488-08 (to V. M.-Y. L.) and NS081033 (to E. J. P.), the Ofer Nemirovsky Family Fund, and the University of Pennsylvania. The authors declare that they have no conflicts of interest with the contents of this article. The content is solely the responsibility of the authors and does not necessarily represent the official views of the National Institutes of Health.
This article was selected as one of our Editors' Picks.
This article contains supplemental Figs S1–S16, Tables S1–S4, and Video S1.
[1] Supported by National Institutes of Health Age-Related Neurodegenerative Disease Training Grant Fellowship T32AG000255.
[2] To whom correspondence should be addressed: 3600 Spruce St., 3 Maloney Bldg., Philadelphia, PA 19104. E-mail: vmylee@upenn.edu.

[3] The abbreviations used are: α-syn, α-synuclein; STED, superresolution stimulated emission depletion; MAP, microtubule-associated protein; pff, preformed fibril; CHQ, chloroquine; mSyn, mouse α-syn; LDH, lactate dehydrogenase; HSPG, heparan sulfate proteoglycan; pTd, post-transduction; DAB, 3,3′-diaminobenzidine; p-syn, phospho-synuclein; DPBS, Dulbecco's phosphate-buffered saline without magnesium and calcium; TB, trypan blue; EGFP, enhanced green fluorescent protein; NAC, non-amyloid component.

widely used to quench fluorescence of extracellular green and red fluorophores, and it does not appreciably cross the plasma membrane over short time courses (<30 min) (16–18).

Herein, we develop and validate an assay using fluorescently labeled α-syn pffs in conjunction with the membrane-impermeable fluorescence quencher trypan blue to selectively image internalized α-syn fibrils under a number of conditions, allowing for the quantitative characterization of concentration dependence, time course, and inhibition of uptake by cultured primary neurons. Using pffs labeled site-specifically with differentially responsive environmental fluorophores, we present evidence that internalized α-syn seeds are rapidly acidified along the endolysosomal pathway, where the majority of material remains for days after uptake. Further, we employ the lysosomotropic weak base chloroquine (CHQ) as a simple model of lysosomal dysfunction. We observe perturbations in endocytic processing of intercellular α-syn seeds after uptake, leading to an acceleration of recruitment of endogenous α-syn, as determined by total pathological α-syn and further visualized by high-resolution imaging of pff seeds in direct interaction with endogenous α-syn. Taken together, these results highlight the endolysosomal system as a major fate of transmitted proteopathic α-syn in primary neurons and suggest that only a distinct minority of internalized seeds escape the endocytic pathway to template recruitment of endogenous α-syn into pathological aggregates. The endolysosomal pathway is probably protective against transmission of proteopathic α-syn seeds and may represent a general therapeutic target for modifying the progression of neurodegenerative diseases.

Results

Trypan blue completely quenches the fluorescence of syn–GFP preformed fibrils

Trypan blue is widely used in cell culture applications as a vital stain due to its polarity and as a fluorescence quencher capable of accepting energy from the excited state of fluorophores through dipole–dipole interactions (16–18). Additionally, trypan blue is a structural analog of the reported amyloid-binding dye Congo red (Fig. 1*A*) and is reported to have an affinity for the amyloid fold (19). We set out to examine the ability of trypan blue to quench fluorescence of pffs generated from recombinant mouse α-syn–His_6-GFP (mSyn–GFP). mSyn–GFP pffs were originally chosen for our initial studies because recombinant mSyn–GFP is readily prepared using established protocols (20), and the C-terminal GFP tag is known not to interfere with aggregation (21, 22). To determine the optimal trypan blue concentration for quenching of mSyn–GFP pffs, we treated a constant concentration of sonicated mSyn–GFP pffs with increasing concentrations of trypan blue and demonstrated >99.95% total fluorescence quenching at 500 μM trypan blue, confirming that the vast majority of GFP moieties are quenched at this concentration (Fig. 1*B*).

We next set out to confirm quenching by microscopy. Poly-D-lysine–coated MatTek dishes were treated for 1 h with sonicated mSyn–GFP pffs and were imaged as serial confocal *z*-sections before and immediately after (<15 min) application of 500 μM trypan blue to establish unquenched and quenched fluorescence levels. Similar dishes containing primary hippocampal neurons were treated with PBS (vehicle control) and imaged to establish autofluorescence levels. Mean fluorescence intensities of pffs in contact with trypan blue were significantly reduced; indeed, the fluorescence intensity was similar to autofluorescence of untreated neurons (Fig. 1*C*). As such, it was determined that independent thresholds for quantifying intracellular objects within each uptake experiment should be determined by relationship to the autofluorescence from PBS-treated neurons, such that no significant signal contribution from unquenched fibrils or cellular autofluorescence would be identified in each image frame. It was empirically determined that a threshold defined at 10× mean autofluorescence excludes signal contribution from both cellular autofluorescence and trypan blue-quenched extracellular pffs.

Brief treatment with trypan blue is not significantly toxic to primary neurons

To assess potential toxicity of trypan blue at concentrations necessary for quenching and treatment times required for imaging, we undertook a pulse–chase experiment utilizing a brief exposure of primary hippocampal neurons to trypan blue followed by a complete wash and medium exchange and measured toxicity 24 h post-treatment. Measurement of lactate dehydrogenase (LDH) release (Promega) at 24 h following a brief 30-min exposure to trypan blue (500 μM) indicates no significantly higher toxicity affected by trypan blue compared with a PBS wash control (Fig. 1*D*). Furthermore, bulk metabolic activity of the culture as assayed by alamarBlue® (Thermo Fisher) reduction shows no significant difference between trypan blue– and PBS-treated controls (Fig. 1*D*). Taken together, these results indicate that a brief treatment with trypan blue is not acutely toxic to primary neurons.

Transduction of neurons with mSyn–GFP pffs and quantification of uptake by quenching extracellular pffs

Treatment of primary mouse hippocampal neurons with 1.5 μg/dish mSyn–GFP pffs for 1 h results in a layer of insoluble mSyn–GFP pffs accumulating on surfaces of the dish as well as on the plasma membrane of neurons (Fig. 1*E*). The amount of mSyn–GFP pffs added to each culture dish was chosen to be consistent with equivalents of α-syn previously optimized in neuronal transductions using unlabeled α-syn pffs (23). To distinguish intracellular from extracellular labeled puncta, trypan blue (500 μM) was applied to the culture dish. Serial confocal *z*-sections reveal the presence of mSyn–GFP puncta contained both in processes and cell bodies (Fig. 1*E*, *left*), indicating rapid uptake by the neuron. Trypan blue fluorescence in solution is suppressed through twisted intramolecular charge transfer quenching, although when bound to protein, trypan blue fluoresces with excitation ~620, emission ~650 nm. As such, trypan blue provides a fluorescent label of the plasma membrane when interacting with extracellular membrane-bound proteins, affording visual confirmation of the boundaries of each cell when serially acquired GFP and trypan blue frames are overlaid (Fig. 1*E*, *right*). These results represent the first time that intracellular mSyn–GFP pff puncta have been quantitatively imaged in both neuronal somata and processes with confocal resolution and no signal contribution from extracellular pffs.

Validation of trypan blue quenching for quantitative measurement of α-syn pff uptake

To validate the method of fluorescence quenching for determining pff uptake and to better understand the mechanisms by which cultured primary neurons take up proteopathic seeds, inhibition of pff uptake was measured under different conditions. First, neurons were transduced with mSyn–GFP pffs at 4 °C for 60 min, and fluorescence signal was compared with neurons transduced at 4 °C for 30 min followed by a 30-min incubation at 37 °C. After 60 min at 4 °C, a layer of pffs had

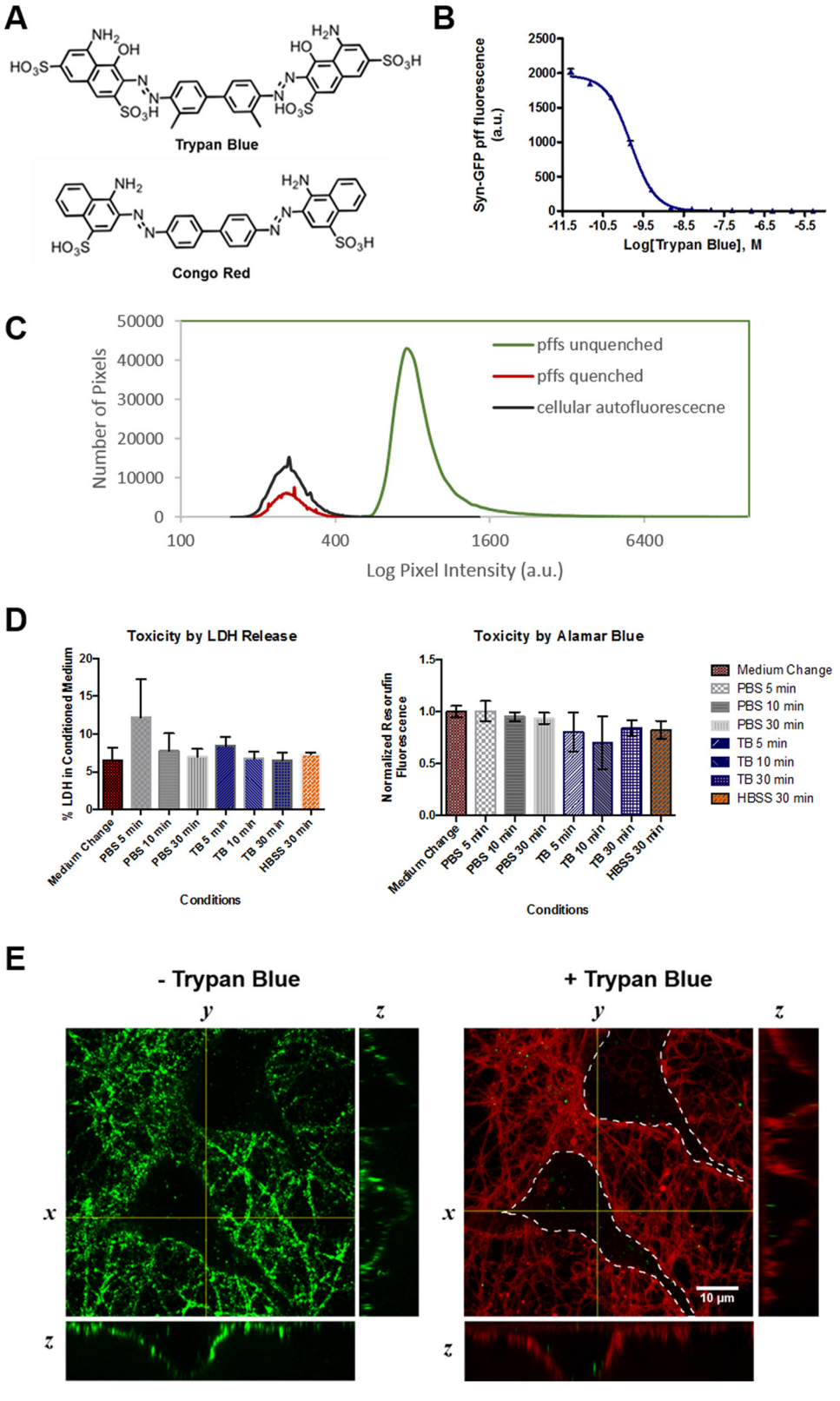

coated neuronal membranes and surfaces of the dish. Upon the addition of trypan blue, the majority of these puncta were quenched, indicating a reduction of uptake (Fig. 2*A*). Inhibition of uptake by continuous incubation at 4 °C relative to the warmed control was found to be 98.5 ± 0.5% (Fig. 2, *A* and *B*; mean ± S.D., $n = 3$), strongly implicating an energy-dependent mechanism of translocation across the membrane, consistent with endocytosis and inconsistent with direct membrane permeation. It has been suggested that pff uptake can be mediated by heparan sulfate proteoglycans (HSPGs) and that preincubation of pffs with heparin inhibits pff binding to cell surface HSPGs via competitive inhibition, resulting in decreased pff uptake (11). Indeed, pretreatment of pffs with 200 μM heparin for 12 h prior to transduction inhibited both cell surface binding and uptake. pff uptake was reduced by 83.2 ± 1.5% (mean ± S.D.) relative to the uninhibited control (Fig. 2, *C* and *D*). Additionally, sonication of pffs was found to be required for robust uptake. Treatment of neurons with unsonicated pff suspensions showed a 68.6 ± 15.4% (mean ± S.D.) reduced uptake at 1 h compared with a sonicated control (Fig. 2, *E* and *F*), suggesting size gating at the membrane consistent with previous reports of tau pff systems (12, 13). Thus, it was found that uptake is contingent on a number of factors, including endocytic activity, membrane surface binding, and fibril size. These inhibition results additionally validate trypan blue quenching of extracellular fluorescent pffs as an appropriate method to determine pff uptake under a number of conditions.

To further characterize pff uptake into primary neurons, we established a dose–response relationship at 1 h post-transduction (pTd). Transduction of neurons with increasing concentrations of mSyn–GFP pffs resulted in a dose-dependent increase of detectable intracellular mSyn–GFP–positive puncta (EC_{50} = 1.81 ± 0.36 μg/coverslip, mean ± S.D.; Fig. 2, *G* and *H*). Interestingly, uptake appears saturable, suggesting a facilitated rather than nonspecific mechanism of uptake.

Trypan blue facilitates the measurement of pff uptake time course

We next set out to characterize the time course of mSyn–GFP pff uptake into primary hippocampal neurons by using trypan blue to unambiguously distinguish intracellular from extracellular mSyn–GFP signal. Transducing primary neurons on day 7 *in vitro* with 1.5 μg of mSyn–GFP pffs/14-mm dish and imaging in the presence of trypan blue at different times pTd provides a biphasic curve indicating uptake and loss of signal (Fig. 3, *A* and *B*). Neurons were first imaged immediately after transduction with a trypan blue treatment ~3 min pTd. By this time, a small amount of intracellular objects are visible (4.4 ± 1.4 objects/frame, mean ± S.D.). Uptake increases thereafter, with 279.1 ± 87.6 objects detectable after 15 min, followed by an apparent plateau at 60 min pTd (677.6 ± 114.2 objects, mean ± S.D.). By 24 h pTd, there is a significant loss of signal, because only 188.3 ± 38.2 objects are detected (mean ± S.D.), indicating either photophysical quenching of GFP fluorescence (at pH <6.0) (24) in progressively acidifying compartments or the beginning of proteolytic lysosomal degradation of mSyn–GFP. This observation is consistent with previous studies using traditional biochemical approaches or microfluidic chamber imaging systems, (15, 25) with additional advantages of quantitative whole-culture imaging with both spatial and temporal resolution of intracellular puncta. By 2 days pTd, few objects are detectable, indicating either robust degradation or pH-dependent fluorescence quenching of intracellular mSyn–GFP seeds. The half-life of signal loss after batch transduction as defined by decrease of detectable GFP puncta was calculated to be 15.9 ± 2.1 h (mean ± S.D.; Fig. 3*C*). To confirm lysosomal processing of mSyn–GFP puncta upon endocytosis, we transfected primary neurons with LAMP1–RFP and examined colocalization. Indeed, mSyn–GFP puncta localize to lysosomes within the first 12 h of pff treatment, and this colocalization is lost as mSyn–GFP signal is reduced, strongly suggesting that mSyn–GFP pffs are processed in lysosomes (supplemental Fig. S12). Sequential extraction of cellular lysate collected at 5 days pTd into Triton X- and SDS-containing buffers followed by Western blot analysis indicates little detectable truncation of mSyn–GFP pffs, although the quantity is reduced compared with a pff control equal to the relative amount of material added to each well. It is unclear whether the measured population reflects mostly intracellular or extracellular mSyn–GFP, because both would be present in the lysate (supplemental Fig. S13).

Additionally, dynamics of intracellular puncta can be recorded for brief time periods in living cells shortly after pff treatment (supplemental Video S1).

pffs persist within the cell for days after initial uptake

The sensitivity of the GFP fluorophore to both pH and proteolytic degradation provides utility as a loss of signal probe for determining initial stages of endocytic or autophagic clearance of mSyn–GFP pffs, although the ultimate fate of intracellular pffs in neurons cannot be determined using this label, because

Figure 1. Trypan blue effectively quenches fluorescence of extracellular exogenously applied mSyn–GFP pffs, allowing for quantitative assessment of pff uptake in primary neurons. *A*, trypan blue is a structural analog of the amyloid binding dye Congo red. *B*, concentration dependence of trypan blue quenching of mSyn–GFP pff fluorescence (25 μg/ml mSyn–GFP). *C*, histograms from representative confocal images of unquenched mSyn–GFP pffs, quenched mSyn–GFP pffs, and cellular autofluorescence of PBS vehicle-treated primary hippocampal neurons (day 7 *in vitro*). For each imaging experiment in this study, a threshold was generated from a multiple of the mean cellular autofluorescence of control cells. *D*, trypan blue is not acutely toxic to primary hippocampal neurons 24 h following brief treatments. *Left*, a pulse– chase experiment measuring LDH release into conditioned medium 24 h after trypan blue (500 μM) or PBS (vehicle) treatments shows no significant toxicity of trypan blue at any time compared with PBS (vehicle), Hanks' balanced salt solution (100%), or cells subjected to a simple medium exchange. *Right*, similarly, metabolic activity assessed by alamarBlue® (resazurin, Thermo Fisher) reduction in the same cultures shows negligible toxicity at 30 min of treatment. *Error bars*, S.D. of triplicate treatments. *E*, upon transduction of primary hippocampal neurons with mSyn–GFP pffs, the insoluble pffs gradually settle to the bottom of the dish, coating the surface and neurons (*left*, spinning disc confocal image; λ_{ex} = 488 nm, λ_{em} = 500–550 nm), where it is impossible to distinguish intracellular from extracellular populations. Application of 500 μM trypan blue (*right*) immediately and quantitatively quenches fluorescence of extracellular pffs, allowing for specific and quantitative identification of intracellular mSyn–GFP puncta. Overlaid together with the 488 nm image is an image of trypan blue (TB) fluorescence as a marker of cellular morphology (λ_{ex} = 561, λ_{em} = 580–653 nm). The *dotted line* has been drawn in to guide the eye in distinguishing cell bodies (interior) from processes and extracellular space (exterior). Orthogonal projections of the confocal *z*-stacks are presented *below* and to the *left* of each image.

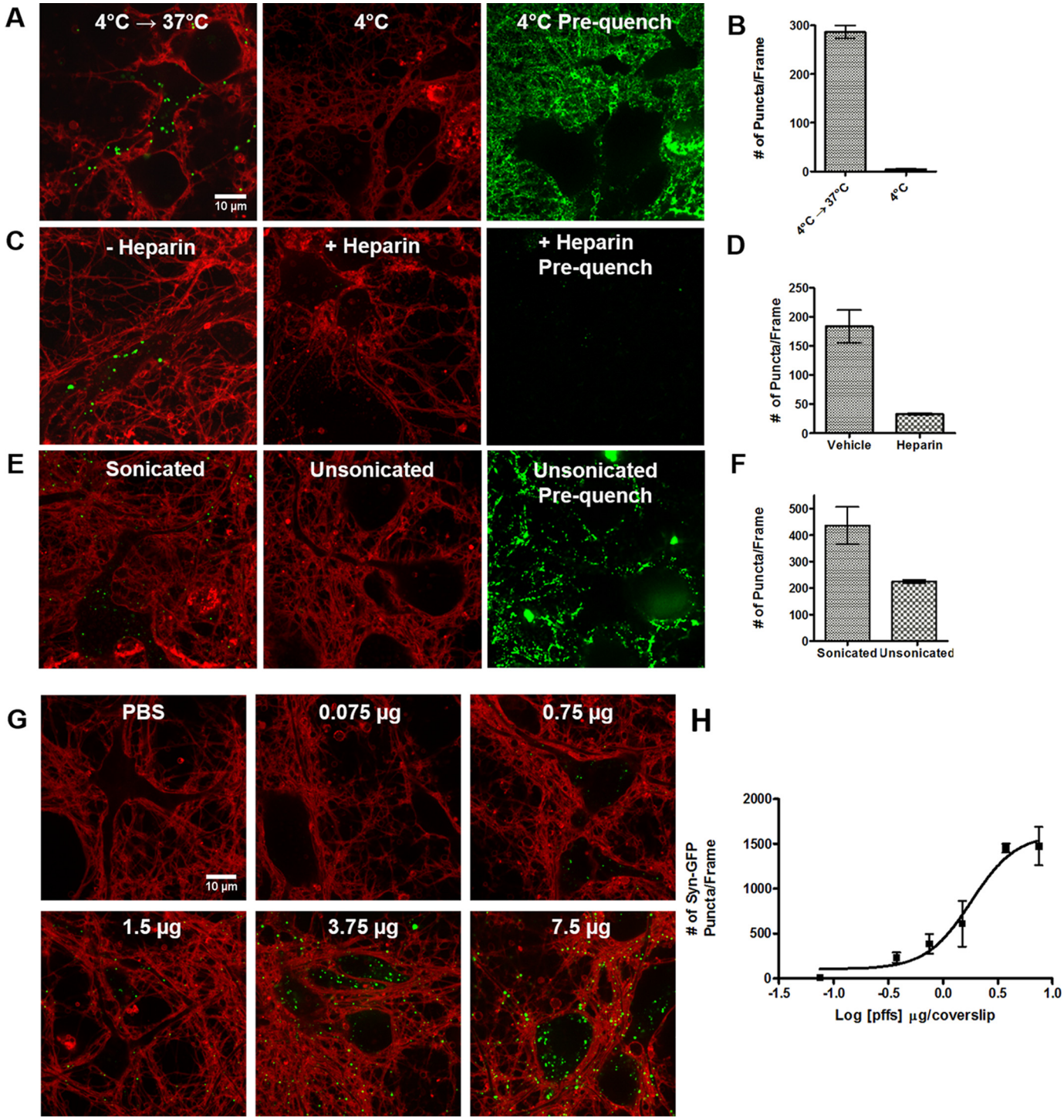

Figure 2. Inhibition of mSyn–GFP pff uptake is quantifiable by trypan blue quenching. *A* and *B*, brief transduction of neurons with mSyn–GFP pffs at 4 °C (30 min) allowed insoluble pffs to settle and interact with neurons. Cultures were then warmed to 37 °C (*left*, uptake control) or maintained at 4 °C for an additional 30 min (*center*), before intracellular puncta were imaged. By 60 min at 4 °C, pffs have settled onto the neurons and surfaces of the dish (*right*). Inhibition of uptake by maintenance at 4 °C was determined to be 98.5 ± 0.5% (mean ± S.D. (*error bars*), $p < 0.0001$, $n = 3$) relative to the warmed control. *Pre-quench*, images of the same field taken immediately before application of trypan blue. *C* and *D*, pretreatment of pffs with heparin (200 μM) overnight followed by co-treatment with 100 μM heparin during transduction resulted in inhibition of uptake by 83.2 ± 1.5% (mean ± S.D., $p = 0.0332$, $n = 2$) relative to vehicle control. *E* and *F*, sonication of mSyn–GFP pffs is required for robust uptake. Uptake of unsonicated pffs was reduced by 68.6 ± 15.4% (mean ± S.D., $p = 0.0395$, $n = 3$) relative to sonicated control. *G* and *H*, pffs are taken up by neurons via a concentration-dependent, saturable mechanism. Trypan blue facilitates quantitation of uptake of increasing concentrations of mSyn–GFP pffs at 1 h pTd in primary hippocampal neurons (day 9 *in vitro*). Uptake becomes saturable at high [pffs], suggesting a limited capacity for uptake, consistent with endocytosis. The EC_{50} of uptake was determined to be 1.8 μg/coverslip ($n = 4$ independent transductions). Results were fit to the four-parameter logistic equation in GraphPad Prism version 4: $Y = \text{bottom} + (\text{top} - \text{bottom})/(1 + 10\ ((\log EC_{50} - X) \times \text{Hill slope}))$, where X represents the logarithm of the pff amount, and Y is the measured response.

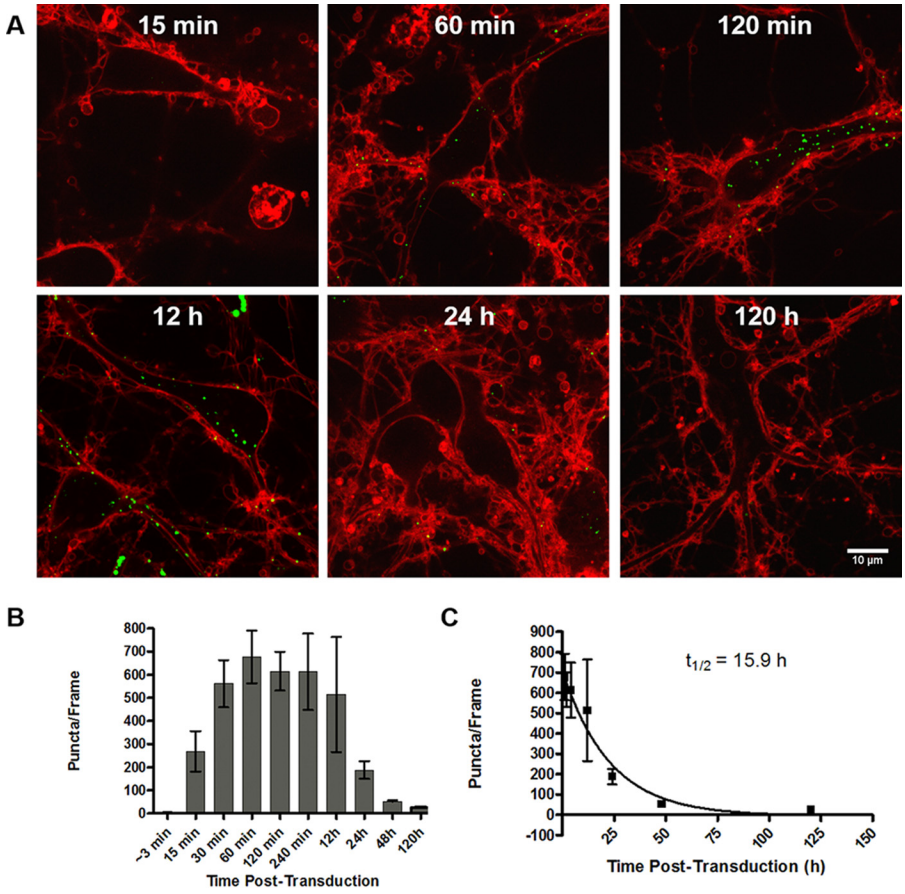

Figure 3. Temporal dynamics of intracellular mSyn–GFP pffs: time course of uptake and loss of fluorescence. *A*, representative images of mSyn–GFP puncta detected after TB quench at increasing times pTd. *B*, quantification of mSyn–GFP puncta in *z*-stacks reveals an initial burst of uptake rapidly after pff treatment with the quantity of puncta per frame plateauing by 60 min pTd. By 24 h, detectable intracellular puncta are reduced by 72.2% compared with 60 min. *C*, the half-life of degradation was determined to be 15.9 h calculated from the initial plateau 60 min pTd. All quantifications represent a mean of five independent experiments ± S.D. (*error bars*).

seeding events generally begin days after transduction (23). To extend the window through which intracellular pffs can be detected, we have generated mutant constructs of both mouse and human α-syn E114C labeled with the environmentally insensitive fluorophore BODIPY (α-S-C^{Bdp}_{114}; Fig. 4*A*) (26–28). This labeling scheme is attractive, given the proximity of amino acid residue 114 to the NAC, the lack of steric interference with recruitment *in vitro* or in primary neurons, and the internal position relative to C-terminal truncation sites (28). α-syn E114C was purified from bacterial culture and labeled with BODIPY maleimide at position 114 (supplemental Figs. S1–S4 and Tables S1 and S2). We found that the presence of the label does not interfere with membrane association, as determined by circular dichroism spectroscopy of α-syn monomer in the presence of SDS micelles (supplemental Fig. S5). Additionally, the label does not perturb fibrillization, as determined by Congo red analysis of aggregation kinetics (supplemental Fig. S6 and Table S3), sedimentation analysis (supplemental Figs. S7 and S8), and transmission electron microscopy (supplemental Figs. S9 and S10 and Table S4). Importantly, pffs generated from 100% α-S-C^{Bdp}_{114} monomer have intracellular seeding capacity similar to that of WT pffs, as evidenced by a concentration dependence comparison with human WT α-syn pffs (supplemental Fig. S11), and are similarly quenched by trypan blue in uptake experiments (Fig. 4, *B* and *C*). Detailed information regarding synthesis, purification, characterization, and validation of E114C-labeled pffs can be found in the supplemental data.

We set out to compare the time course of uptake and intracellular persistence of α-S-C^{Bdp}_{114} pffs with those of mSyn–GFP pffs. Both mouse and human α-syn E114C-labeled pffs were tested in our uptake assay to characterize any potential differences in behavior between species. Indeed, detectable mouse and human α-S-C^{Bdp}_{114} puncta persist at least 1 week pTd (Fig. 4, *B–E*). In fact, α-S-C^{Bdp}_{114} signal persists for days longer than GFP signal, due to the pH insensitivity of the appended BODIPY-FL fluorophore. Interestingly, no significant differences in uptake and intracellular persistence were observed between mouse and human pffs.

pffs are mostly trafficked to lysosomes after initial uptake

To characterize the environment around intracellular α-syn puncta at different times pTd, we generated dual-labeled pffs from 85% α-S-C^{Bdp}_{114} and 15% monomer labeled with the pH-sensitive rhodamine analog pHrodo red (α-S-C^{pHR}_{114}). pHrodo red is widely used to study endocytosis due to its favorable pH-sensitive photophysical properties, displaying little fluorescence at neutral pH and fully unquenched fluorescence in acidic environments (29). Using the same quenching-based

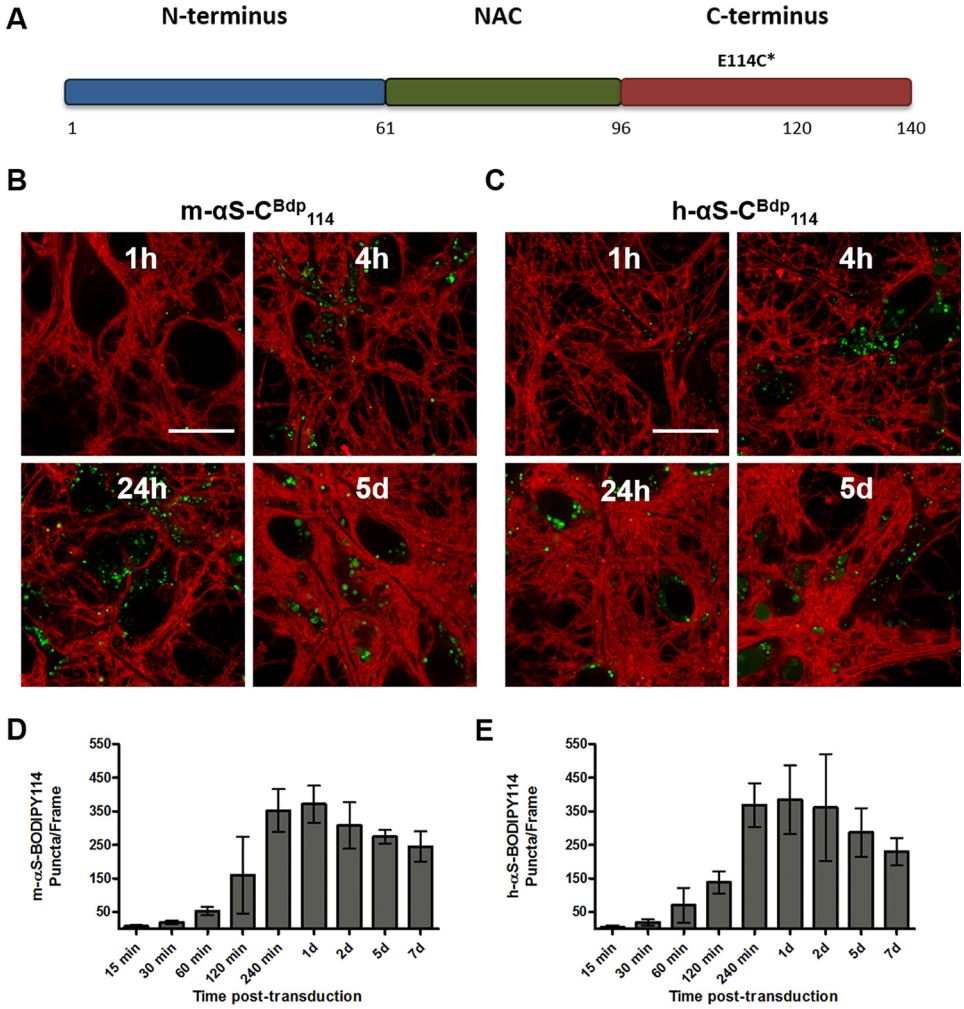

Figure 4. A pH-insensitive label close to the NAC reveals persistence of pffs within cells. *A*, a schematic illustrating the label site on E114C α-syn, internal to the c-terminal caspase cleavage site between amino acids 120 and 121 and spatially separated from the NAC (amino acids 61–95). Representative images of m-αS-C$^{Bdp}_{114}$ pffs (*B*) and h-αS-C$^{Bdp}_{114}$ pffs (*C*) immediately after TB treatment indicate days-long intracellular persistence of internalized pffs. *Scale bar*, 20 μm. *D* and *E*, quantification of m-αS-C$^{Bdp}_{114}$ ($n = 3$) and h-αS-C$^{Bdp}_{114}$ ($n = 5$) uptake and continued intracellular presence. *Error bars*, S.D. of the means of independent experiments as indicated.

imaging techniques as above, we can observe the relative proportion of internalized pffs in the late endocytic pathway via quantitative comparison of puncta positive for BODIPY alone with those positive for both BODIPY and pHrodo; acidified pffs in late endosomes or lysosomes would fluoresce both green and red, whereas pffs in early endosomes or outside the endocytic pathway entirely should only fluoresce green. By imaging a time course of these dual-labeled pffs, it is evident that pffs are acidified rapidly after internalization by neurons (Fig. 5, *A* and *B*). Indeed, the percentage of dual-fluorescent puncta increases from 26.6 ± 8.3% at 2 h pTd to 54.9 ± 9.6% at 4 h pTd, with 84.9 ± 7.9% of all puncta displaying dual fluorescence by 24 h pTd, indicating that the vast majority of pffs are in acidified late endosomes or lysosomes (mean ± S.D.), as determined by an object-based colocalization analysis (Fiji). At 7 days pTd, that proportion of co-labeled objects increases to 94.6 ± 3.5%. Thus, it appears that the vast majority of pffs taken up by the neuron pass through the endocytic pathway, remaining therein.

Additionally, using pffs generated from 100% αS-C$^{Bdp}_{114}$, which remain detectable within the cells 24 h pTd (Fig. 4), we performed uptake imaging experiments on Lysosome-associated membrane protein 1–RFP (LAMP1–RFP)–transfected neurons. At both 24 and 72 h post-transduction, it is evident that the majority of intracellular punctate signal in LAMP1-expressing neurons is contained within LAMP1–RFP–positive structures (Fig. 5*C*). Finally, to confirm the intracellular persistence of pffs for days post-transduction, we examined human WT α-syn pff uptake at the EM level at 7 days pTd through immunostaining with the human α-syn–specific antibody Syn 204 (Fig. 5*D*). We observed considerable human α-syn immunoreactivity within endocytic organelles, as detected by areas of 3,3′-diaminobenzidine (DAB) deposition. Thus, using a different detection method with ultrastructural resolution, we demonstrate that α-syn is retained in the endolysosomal system. These results are consistent with the observation that punctate BODIPY and pHrodo red signal indicate the persistence of α-syn within the endocytic pathway for days after uptake. Additionally, we observed the presence of αS-C$^{Bdp}_{114}$ pffs 4 h pTd by DAB (supplemental Fig. S15, *A* and *B*), confirming that the pffs exist within the endocytic pathway at early time points. Nanogold detection further reveals the fibrillar nature of endocytosed species (supplemental Fig. S15, *C–E*).

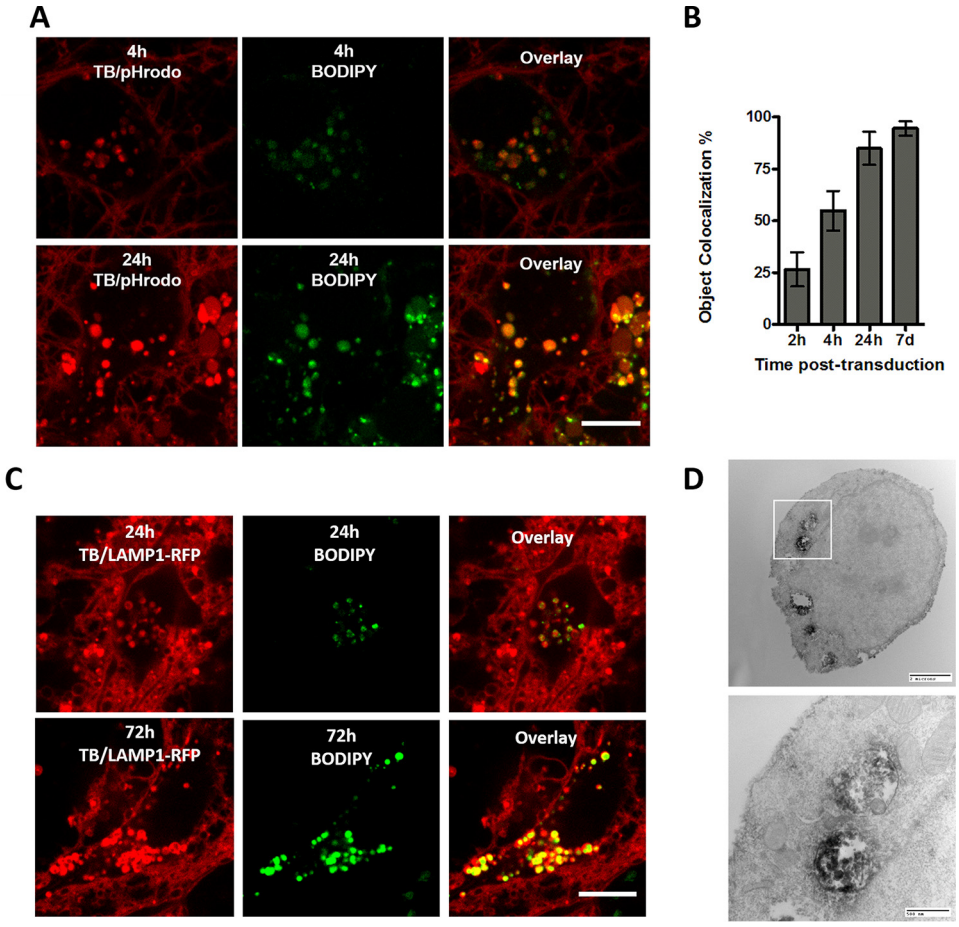

Figure 5. pffs are rapidly localized to the endocytic pathway after uptake. *A*, dual-labeled α-syn pffs generated from 85% αS-C^{Bdp}_{114} monomer and 15% αS-C^{pHR}_{114} monomer indicate the progressive acidification of pffs after uptake, consistent with endocytic trafficking. *Scale bar*, 10 μm. Images are representative of four replicates. *B*, quantification of the percentage of BODIPY-positive internalized puncta displaying red fluorescence from pHrodo red acidification in the late endocytic pathway, as determined by ImageJ JACoP object-based colocalization. *C*, expression of LAMP1–RFP in primary mouse hippocampal neurons followed by transduction with αS- C^{Bdp}_{114} pffs indicates highly lysosomal localization of internalized pffs at 24 h (*top*) and 72 h (*bottom*) pTd. *Left*, representative images of LAMP1–RFP and trypan blue fluorescence. *Center*, intracellular αS-C^{Bdp}_{114} signal in the same field. *Right*, overlay, indicating that intracellular αS-C^{Bdp}_{114} signal is largely localized to lysosomes. *D*, immuno-EM of human WT α-syn pffs on day 7 pTd confirms the prolonged endocytic localization of exogenous synuclein species. Detection was carried out with the human α-syn-specific antibody Syn 204 (epitope: residues 87–110), followed by treatment with horseradish peroxidase–conjugated secondary antibody and subsequent DAB oxidation. Images are a representative sampling of cells from six coverslips transduced in parallel. The *highlighted square above* represents the region of interest imaged at higher resolution *below*. *Error bars*, S.D.

Brief perturbation of lysosomes leads to an increase in detectable mSyn–GFP puncta 24 h post-transduction

α-Syn pffs have been shown to at least partially localize to lysosomes in the hours following transduction in model cell lines and neurons (14, 15, 30). In this context, our results indicate that the majority of the intracellular pffs are localized in the endocytic pathway shortly after transduction (Fig. 5). Because lysosomal dysfunction has been implicated in neurodegenerative synucleinopathies, we asked whether brief disruption of lysosomal activity would result in an increased proportion of exogenous pffs resisting endolysosomal sequestration or degradation. The lipophilic weak base CHQ is a widely used as a nonspecific inhibitor of lysosomal hydrolases by collapsing the pH gradient across the lysosomal membrane; the resulting alkalinization inhibits pH-dependent hydrolases. CHQ has previously been used to enhance efficiency of DNA transfections by suppressing lysosomal degradation of exogenously applied nucleic acids (31–34) and has been suggested to inhibit degradation of α-syn pff species (35). Furthermore, CHQ has been shown to cause dilation of lysosomes (36, 37) as well as disruption of lysosomal membranes (38, 39). In light of our results suggesting the endocytic location of exogenously applied α-syn fibrils (Figs. 3 and 5), we asked whether brief treatment with CHQ shortly after transduction with pffs would result in an increase in mSyn–GFP puncta at 24 h compared with a vehicle-treated control. To measure either retardation in endocytic processing or outright escape from the endocytic pathway, we exploited the pH and proteolytic sensitivity of GFP, which we hypothesized would afford an increased detectable population of intracellular mSyn–GFP puncta at 24 h pTd, either through escape from the endocytic pathway or decreased acidification and/or proteolytic degradation of the fluorophore in damaged lysosomes. Indeed, when neurons are transduced for 3 h with mSyn–GFP pffs followed by a brief treatment with the lysosomotropic CHQ (100 μM, 30 min) and extensive washing, the number of mSyn–GFP puncta increased from 56.0 ± 24.6 to 202.5 ± 60.1 (Fig. 6, *A* and *B*; untreated and CHQ treated, respectively; mean ± S.D.; $n = 3$ independent transductions of

two plates each; $p = 0.0174$; Student's t test). The observed increase in mSyn–GFP puncta at 24 h in response to CHQ treatment confirms the endocytic pathway as a major fate of exogenously applied proteopathic seeds after uptake by neurons. This is supported by a similar experiment employing pffs generated from 85% αS-C^{Bdp}_{114} and 15% αS-C^{pHR}_{114}. It was found that signal colocalization between pHrodo red and BODIPY was significantly decreased in CHQ-treated cultures 24 h after transduction, indicating that pffs are exposed to less acidic environments (supplemental Fig. S14, *A* and *B*). Importantly, CHQ treatment did not seem to have an effect on 85% αS-C^{Bdp}_{114}, 15% αS-C^{pHR}_{114} pff uptake, because the total number of BODIPY-positive puncta was unchanged compared with vehicle control (supplemental Fig. S14*C*). Whether the prolonged signal of mSyn–GFP and the decreased colocalization of αS-C^{pHR}_{114} with αS-C^{Bdp}_{114} result from residual chemical

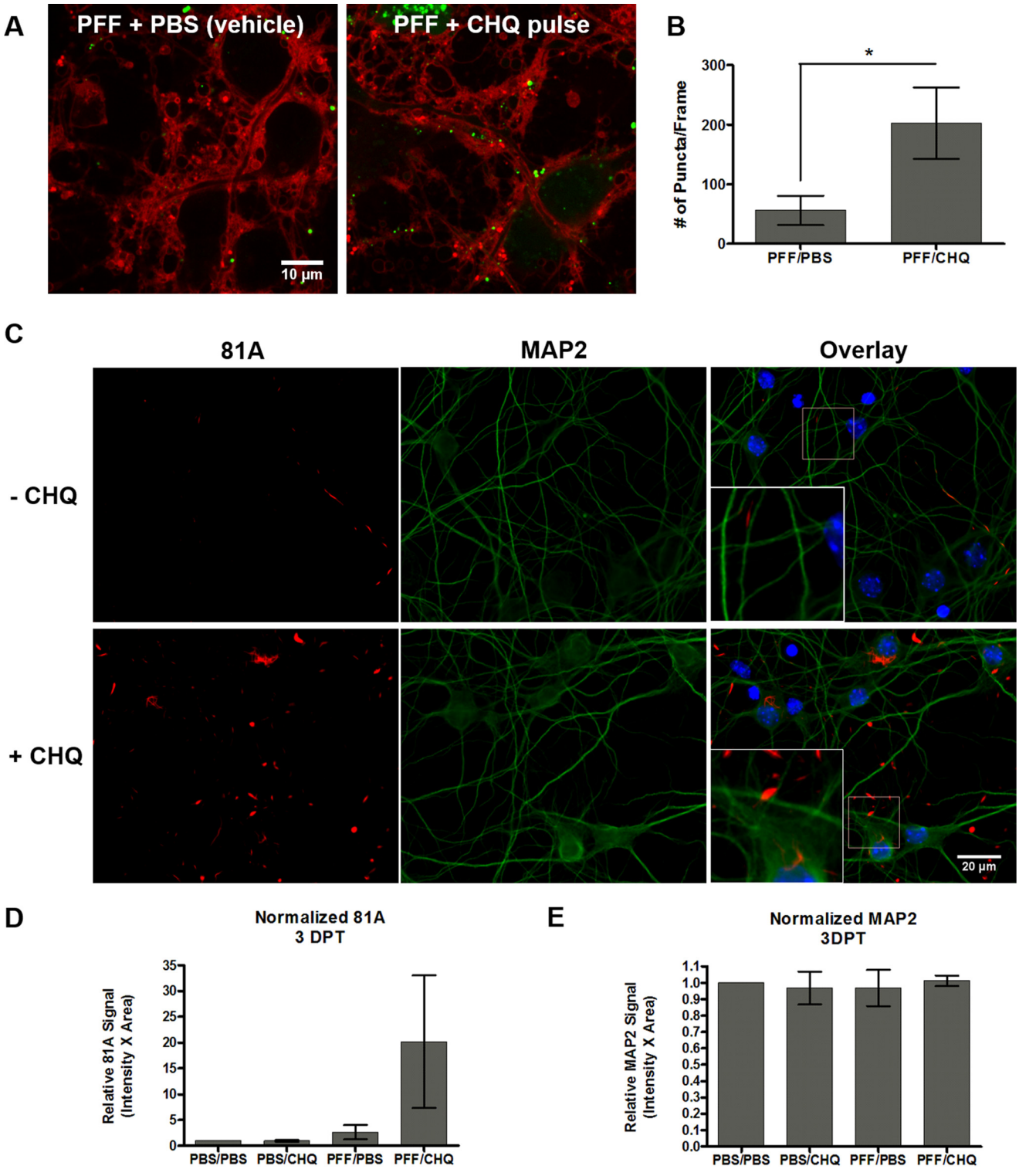

alkalinization of acidic compartments, perturbation of those organelles (*e.g.* lysosomal swelling or rupture), or direct escape, CHQ affects lysosomal processing of exogenous seeds. These experiments demonstrate the ability to directly observe and interrogate the efficiency and impairment of lysosomal processing of fluorescently labeled α-syn seeds after uptake without a background contribution from extracellular exogenous protein.

Brief perturbation of lysosomes leads to an acceleration of intracellular inclusion formation and recruitment

We then asked whether the increase in detectable intracellular mSyn–GFP seeds after CHQ treatment leads to an acceleration in recruitment of endogenous α-syn relative to pff-treated control. Treatment of neurons with pffs for 3 h followed by a brief CHQ pulse (100 μM, 30 min) and subsequent incubation for 72 h resulted in a significant increase in the amount of p-syn (Ser(P)-129; antibody 81A)-positive inclusions, as determined by quantitative immunofluorescence. The extent of aggregation was quantified by both signal area and fluorescence intensity on whole coverslips using a slide scanner (PerkinElmer Life Sciences). pff treatment alone followed by extensive washing and incubation with PBS vehicle control resulted in a small amount of pathology (Fig. 6, *C* and *D*; 2.63 ± 1.19-fold, mean ± S.D./PBS control; $n = 4$) by day 3, consistent with previous reports (20, 23). Treatment with a brief CHQ pulse shortly after pff transduction resulted in a significant increase in pathology, to 20.17 ± 11.12-fold (Fig. 6, *C* and *D*; mean/PBS control ± S.D.; $n = 4$; $p < 0.01$ compared with PBS/PBS control, $p < 0.05$ compared with pff/PBS control). Brief CHQ treatment had no deleterious effect on morphology of the somatodendritic compartment, as determined by total microtubule-associated protein 2 (MAP2) staining on the same coverslips 3 days after treatment (Fig. 6, *C* and *E*). Additionally, CHQ treatment alone had no effect on p-syn aggregation or MAP2 morphology in parallel cultures not treated with pffs (supplemental Fig. S16).

We next examined colocalization between αS-C^{BdP}_{114} pffs and p-syn inclusions (81A; Ser(P)-129) at 24 h pTd with or without CHQ. Colocalization between p-syn and αS-C^{BdP}_{114} is present in a subset of 81A-positive structures at 24 h pTd in CHQ-treated cells (Fig. 7, *A* and *D*), indicating that compromised lysosomal integrity can lead to accelerated seeding directly by pff seeds. Few p-syn-positive structures are visible at the same time in pff-treated control neurons (Fig. 7, *A* and *D*). By 4 days pTd, p-syn aggregates are detected in pff-treated neurons, and robust p-syn signal is visible in neurons exposed to a CHQ pulse (Fig. 7, *B* and *C*). Colocalization between p-syn and exogenous αS-C^{BdP}_{114} seeds is evident in a subpopulation of inclusions only in pff- and CHQ-treated neurons at 24 h and both pff-vehicle– and pff-CHQ–treated neurons by 4 days pTd (Fig. 7, *A* and *B*). Colocalization events are relatively sparse in each (Fig. 7*D*). Seeding and recruitment by αS-C^{BdP}_{114} pffs was observed by superresolution stimulated emission depletion (STED) microscopy (Fig. 7, *E* and *F*), suggesting that colocalization events represent seeded aggregation resulting from exogenous pff species. These data suggest that once recruitment is initiated by a small number of seeds relative to the total intracellular population, the resultant aggregates are probably dynamic in nature, and the recruited endogenous α-syn can fragment from pathological aggregates to further seed additional discrete inclusions. It is entirely possible that the development of intracellular α-syn inclusions in neurons is a result of a relatively small number of seeds escaping endocytic degradation to initiate recruitment.

Discussion

Intercellular transmission of α-syn pathology is now widely considered to be a mediator of the spatiotemporal spread of synucleinopathies in the brain, although a lack of model systems capable of unambiguous visualization of internalized proteopathic seeds has obscured the fate of these seeds in the initial hours and days after uptake. This critical window must be further explored to better understand the biological and chemical processes underlying the development of intracellular pathological aggregates in response to a proteopathic seed. Our studies introduce an experimental system for the quantitative characterization of α-syn pff uptake and intracellular processing in primary neurons under various conditions. We found that the vast majority of internalized α-syn seeds persist in lysosomes for days, suggesting the essential role of endolysosomal integrity in determining the rate of cell-to-cell transmission of α-syn pathology. By modeling lysosomal malfunction during pff treatment, recruitment of pathological aggregates is accelerated, and colocalization with individual BODIPY-labeled pffs can be observed at as little as 1 day pTd. Together, these results suggest that initiation of recruitment is predicated on few individual seeding events even in the presence of large amounts of proteopathic seeds inside the cell.

Determination of neuronal uptake and the immediate fate of seeds has been impeded by a dearth of robust, selective, and quantitative methods. In our hands, the majority of sonicated α-syn pffs remained extracellular following the addition to the neuronal culture medium, probably becoming sequestered by

Figure 6. Brief inhibition of lysosomal activity with CHQ interferes with lysosomal processing of pffs and enhances the recruitment of endogenous α-syn to intracellular inclusions. *A*, representative images of intracellular mSyn–GFP puncta in live neurons 24 h pTd without (*left*) and with (*right*) a brief pulse of CHQ to inhibit lysosomal proteases (30 min, 100 μM). Images were acquired immediately after treatment with 500 μM TB to quench fluorescence of extracellular mSyn–GFP signal. *B*, quantification of detectable intracellular mSyn–GFP puncta after pff transduction (55.9 ± 24.7, mean ± S.D.) compared with pff transduction followed by CHQ pulse (202.5 ± 60.1, mean ± S.D.). *Error bars*, S.D. of three independent experiments, each consisting of transductions performed in duplicate, at least five images per transduction. Statistical significance was determined by Student's *t* test (*, $p = 0.0174$). *C*, immunofluorescence staining of fixed cells 3 days post-transduction with WT mSyn pffs (0.5 μg/coverslip) reveals a substantial increase in the amount of p-syn–positive inclusions (81A; Ser(P)-129) resulting from a 3-h transduction period followed by a 30-min CHQ pulse (+*CHQ*) relative to neurons transduced with pffs followed by a pulse with PBS vehicle (−*CHQ*). No difference in the appearance of neuronal morphology was indicated by staining for MAP2. *D*, >70% of total coverslip surface area was quantified using HALO analysis of scanned coverslips, revealing a 2.63 ± 1.19-fold (mean ± S.D., $n = 4$) increase in signal relative to PBS control (81A background) as a function of pff transduction. A 30-min CHQ pulse applied 3 h pTd increased pathology on day 3 pTd to 20.17 ± 11.12-fold over PBS control (mean ± S.D., $n = 4$, $p < 0.01$ (analysis of variance)). *E*, coverslips quantified using a similar protocol to determine somatodendritic morphology showed no significant changes in MAP2 coverage as a function of any treatment ($n = 4$, analysis of variance).

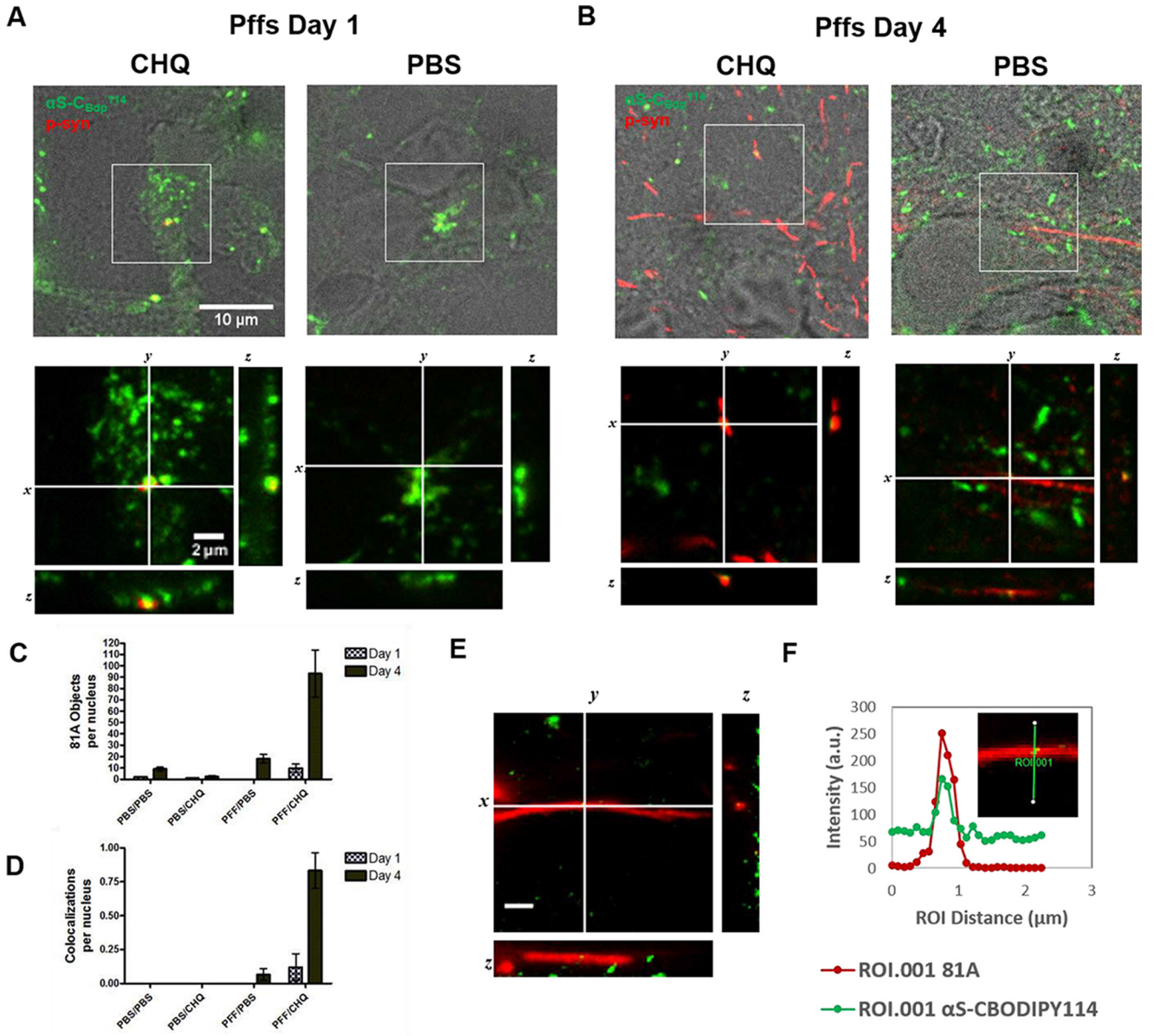

Figure 7. Recruitment and seeding by BODIPY114 pffs can be directly imaged after CHQ treatment. *A*, immunofluorescence analysis of Ser(P)-129 inclusions recruited to αS-C^{Bdp}_{114} seeds (*green*) shows recruitment 24 h pTd after a 30-min CHQ pulse (*left*). p-syn inclusions are detected (*red*), as are individual recruitment events, as indicated by colocalization of p-syn and αS-C^{Bdp}_{114} signal. Control cells transduced at the same time but treated with PBS vehicle show no detectable p-syn inclusions (*right*). *B*, pff and CHQ-treated cells fixed 4 days pTd show a vast increase in the amount of p-syn pathology (*left*). By 4 days pTd, pff-treated cells show a slight increase in the amount of p-syn pathology detected (*right*). Although recruitment events are evident in both conditions, comparably few are detectable compared with the number of Ser(P)-129–positive inclusions. The *top panels* show a single spinning disk confocal *z*-plane overlaid with a corresponding bright field image. *Boxes*, *enlarged* regions of interest presented *below*. Orthogonal projections of the confocal *z*-stacks are presented *below* and to the *left* of each image. *C*, quantification of individual p-syn aggregates normalized to nuclei shows the effects of CHQ on acceleration of recruitment. *D*, quantification of individual colocalization events per nucleus indicates that CHQ increases the amount of detectable recruitment events, although the relative proportion per cell is small regardless of condition. *E*, superresolution STED microscopy indicates that colocalization events indeed represent recruitment of endogenous p-syn-positive aggregates by exogenous αS- C^{Bdp}_{114} pffs at 4 days post treatment with pffs and CHQ. *Scale bar*, 5 μm. *F*, line profile analysis reveals αS-C^{Bdp}_{114} signal within the same Ser(P)-129–positive inclusion (*inset image*, an *enlarged* representation of the same inclusion showing the region of interest (*ROI*) used for line profile analysis). *Error bars*, S.D.

the culture dish itself or remaining too large after sonication for efficient endocytosis. The result is a confounding amount of extracellular signal that is impossible to practically distinguish from intracellular signal. To quantitatively characterize neuronal uptake of pffs and to observe intracellular distribution of proteopathic α-syn seeds, we set out to adapt our pff-induced neuronal synucleinopathy model in conjunction with an uptake assay whereby extracellular fluorophores are quenched via dipole–dipole interaction with a cell-impermeable fluorescence quencher. We were encouraged to observe that a relatively low concentration of trypan blue (500 μM) quenches fluorescence of mSyn–GFP pffs to background cellular autofluorescence levels without inducing significant toxicity to neurons over treatment periods of <30 min, although we were careful to limit imaging of any single culture dish to <10 min. Trypan blue provides a red fluorescent label of the plasma membrane, allowing visual confirmation of the intracellular location of remaining α-syn pff fluorescence. Most importantly, quantifi-

cation of 3D puncta is possible using automated object identification algorithms.

Our results both validate the trypan blue method for measuring uptake and confirm endocytosis as the principal mechanism of pff uptake in primary neurons. First, uptake is significantly inhibited by low temperature, competitive binding of fibrils to heparin, and lack of sonication. Second, saturation of uptake at high concentrations of fibrils also indicates a limited pathway(s) of uptake, consistent with endocytosis.

Using this assay system, we found that lysosomal processing is the major fate of internalized α-syn pffs. After a rapid burst of uptake of mSyn–GFP pffs followed by a plateau period of saturation with respect to the number of intracellular objects, the neurons are largely cleared of fluorescent mSyn–GFP puncta within 24 h. Recognizing the pH and proteolytic sensitivity of EGFP fluorescence, we hypothesized that by 24 h post-treatment, the mSyn–GFP pffs have entered the late stages of the endocytic pathway, where loss of signal is probably due to a complex interplay between proteolytic cleavage and protonation of the GFP fluorophore. By employing the E114C α-syn mutant such that the pH-insensitive fluorophore BODIPY can be labeled specifically at Cys-114, we have shown that α-syn pffs are long-lived within the cells and can be imaged at least 1 week post-treatment. Treatment of neurons with αS-C$^{Bdp}_{114}$ co-fibrillized with a small amount of E114C α-syn labeled with the pH-sensitive endocytic probe pHrodo red (29) indicates that the vast majority of these intracellular puncta are rapidly acidified within hours after initial treatment and largely remain in a low-pH environment for up to 7 days. This is consistent with trafficking along and sequestration in the endocytic pathway. Thus, we have two separate lines of evidence from pH-sensitive fluorophores suggesting acidification of nearly all internalized pffs 24–48 h after pff treatment. Additionally, we observed a high degree of colocalization between αS-C$^{Bdp}_{114}$ puncta with LAMP1–RFP in transfected neurons. Finally, we observe exogenous α-syn pff seeds encapsulated within endocytic compartments from 4 h to 7 d pTd at the EM level. We thus conclude that the bulk of internalized species remain in and are processed by lysosomes for days after internalization.

Along with previous immunofluorescence studies showing a subset of α-syn pffs in lysosomes within 24 h after pff treatment, further evidence from cultured immortalized cell lines has recently surfaced suggesting some extent of vesicular location of pffs shortly after uptake (35, 40). For seeding of endogenous α-syn to occur after uptake by endocytosis, pathogenic species must somehow escape endocytic trafficking and degradation such that they can interact with soluble species and initiate recruitment. Although it has been suggested that large quantities of α-syn fibrils can permeabilize and escape from lysosomes directly, the processes governing this putative escape are still poorly understood (41, 42). Other pathogenic species, particularly oligomers, have also been postulated to directly permeabilize membranes or form membrane-spanning pores (43–45). It has recently been demonstrated that phosphorylation of exogenous α-syn species leads to an increase in lysosomal rupture following endocytosis, which may be a relevant mechanism of pathological α-syn transmission (46). Using sonicated pffs generated from unmodified recombinant α-syn, we did not observe endocytosis-independent mechanisms of uptake in our studies. Under our standard treatment conditions, we could not detect large-scale escape from the endocytic pathway or alkalinization of endocytic organelles, although intracellular seeded aggregation occurs readily as a result of pff treatment.

It has been well established in human post-mortem studies and model systems that genetic defects in endocytic trafficking, lysosomal integrity, and lysosomal hydrolase activity are risk factors for synucleinopathies (25, 47–55). Lysosomal defects are thought to contribute to *de novo* aggregation of α-syn and impaired autophagic degradation of mature cytosolic aggregates (56, 57). Using CHQ to model lysosomal impairment, we measured an increase in the rate of inclusion generation in a seeded aggregation system, suggesting that defects in lysosomal activity and integrity may further accelerate the rate of synucleinopathy transmission. Our seeded aggregation results using αS-C$^{Bdp}_{114}$ show that it is possible to image direct seeding of endogenous α-syn to exogenous pffs, although relatively few intracellular p-syn inclusions contain αS-C$^{Bdp}_{114}$ signal. These results further suggest that recruitment may be initiated by a relatively small number of insoluble species compared with the population sequestered in the endocytic pathway.

Multiple cell-based models have been converging recently on the likely centrality of cell-to-cell transfer of proteopathic seeds in the progression of synucleinopathies, although mechanistic questions remain. It is still unclear whether specific α-syn strains are internalized via distinct receptors or endocytic mechanisms, and different mechanisms of seed uptake could be biased toward distinct fates for the cargo (*i.e.* proteolytic degradation, endocytic escape, trafficking to recycling endosomes, etc.). The recent report of LAG3 as a putative receptor for α-syn uptake is compelling, although multiple receptors or transmission mechanisms for α-syn aggregate internalization are possible (58). For example, it has been demonstrated via flow cytometry that macropinocytotic uptake of both α-syn and Tau by immortalized cells and primary neurons is mediated by HSPGs (11). Tunneling nanotubes have been implicated in transfer of exogenous α-syn pffs as lysosomal cargo between cells in culture (59). Our studies indicate that proteopathic seeds remain in lysosomes for days, providing an extended window for direct cell-to-cell transfer if such mechanisms occur in tissue. Direct release of exogenous pffs from neurons has been demonstrated following treatment in microfluidic culture systems (15). Anterograde and retrograde axonal trafficking of endocytosed α-syn pffs has been observed with the kinetics of slow component b of axonal transport (14). Whether internalized seeds are transported in endocytic organelles or as naked assemblies on microtubules remains an important unanswered question (60). Based on our results, we propose that the majority of intracellular pff-derived seeds remain in the endocytic pathway during axoplasmic transport.

In summary, our studies introduce an experimental system for quantitative characterization of pff uptake and intracellular processing. The selective imaging of internalized α-syn pff species has been validated by inhibition experiments and represents an assay for quantitative analysis of pff uptake into neurons under various conditions. Using pffs labeled with different environmentally responsive fluorophores, we found that α-syn

seeds are sequestered by lysosomes for days post-treatment. By modeling lysosomal impairment for a brief period following pff treatment, recruitment of endogenous α-syn is accelerated and can be observed on a distinct minority of individual BODIPY-labeled pffs in as little as 1 day pTd. If continuous endocytic sequestration and eventual lysosomal degradation of internalized proteopathic seeds are central for staving off the transmission of pathology, disease-associated defects in endolysosomal processing could result in increased seeding of pathology in predisposed patients. Our results suggest that lysosomal integrity may be paramount to protection from transmission of proteopathic synucleinopathies, and targeting lysosomal degradation of transmitted proteopathic seeds could represent a new therapeutic strategy for modifying progression of synucleinopathies or transmissible neurodegenerative diseases in general.

Experimental procedures

Preparation and characterization of fluorophore-labeled pffs

Recombinant full-length mouse WT α-syn linked to EGFP at the C terminus by a His_6 tag (mSyn–GFP) was generated and purified as described previously for human WT α-syn (20, 61). mSyn–GFP pffs were generated by incubating purified α-syn (15 mg/ml in Dulbecco's phosphate-buffered saline without magnesium and calcium (DPBS; Corning Inc.)) at 37 °C with constant agitation for 7 days. Formation of pffs was assayed by sedimentation and EM analysis as described previously (20). E114C mutant α-syn monomer was prepared as described previously and labeled with BODIPY or pHrodo red maleimide dyes, and labeled E114C α-syn was further characterized by MALDI MS, CD, and aggregation kinetic analysis as described previously (28). For detailed synthetic protocols and complete characterization of E114C-labeled pffs, see the supplemental materials.

Primary neuronal culture

Primary neuronal cultures were prepared from embryonic day 15–17 embryos of CD1 mice (Charles River) as described previously (23). All procedures were performed according to the National Institutes of Health Guide for the Care and Use of Experimental Animals and were approved by the University of Pennsylvania institutional animal care and use committee. Dissociated hippocampal neurons were plated onto sterile, poly-D-lysine–coated 13-mm German glass coverslips (Karl Hecht GmbH & Co. KG) in a 24-well plate at 100,000 cells/coverslip for immunocytochemistry experiments or 100,000 cells in the glass center chamber of a MatTek dish (35-mm dish, 14-mm well, number 1.5 coverglass) for live cell imaging and were allowed to mature for 7–10 days in complete neuronal medium (neurobasal without phenol red (Thermo Fisher), 5% B27 supplement (Thermo Fisher)). Medium was partially exchanged every 3–4 days. Toxicity of trypan blue was determined by a pulse–chase experiment. Briefly, neurons were treated for increasing times up to 30 min with 500 μM trypan blue in DPBS, washed thoroughly with complete neuronal medium, and incubated for 24 h. LDH release into the conditioned medium was assayed following the manufacturer's protocol of a commercial colorimetric kit (CytoTox 96®, Promega). Bulk metabolic activity in the culture was determined by the alamarBlue® reduction assay (Thermo Fisher) per the manufacturer's protocol.

General protocol for mSyn–GFP pff transduction and trypan blue quenching

Trypan blue diphosphate (Sigma-Aldrich) solutions were freshly prepared on the day of experiment as a 2× solution (1 mM in DPBS without Ca^{2+}, Mg^{2+}; Gibco) and sterilized by filtration. Trypan blue solution and fresh neurobasal without phenol red, B27, or antibiotic supplementation were equilibrated at 37 °C, 5% CO_2. mSyn–GFP pffs were diluted in DPBS to 300 μg/ml for mSyn–GFP or 100 μg/ml for E114C-labeled mutants and sonicated (Diagenode Biorupter™ UCD-300 bath sonicator set to high, 30-s sonication followed by a delay period of 30 s, 10 min total). For dose–response experiments, serial dilutions were prepared after sonication. Sonicated pffs were then diluted in neurobasal to working concentrations. The neuronal culture dish was then washed gently two times with 2 ml of equilibrated neurobasal to remove B27. After washing, all neurobasal was removed from the dish, and 100 μl of transduction suspensions were directly added to the center chamber. Transductions were allowed to proceed for the indicated time. Transductions longer than 4 h were conducted in equilibrated neuronal medium, which was gently washed and replaced with neurobasal prior to imaging. Immediately before imaging, the volume of transduction medium in the MT dish was increased to 1 ml by adding 900 μl of neurobasal. Images were acquired on a spinning disk confocal microscope equipped with a Yokogawa CSU X1 scan head combined with an Olympus IX 81 microscope. Acquisition and hardware were controlled by MetaMorph version 7.7 (Molecular Devices, Downingtown, PA). An Andor iXon3 897 EMCCD camera (Andor Technology, South Windsor, CT) was used for image capture. Solid-state lasers for excitation (488 nm and 561 nm) were housed in a launch constructed by Spectral Applied Research (Richmond Hill, Ontario, Canada). An Olympus ×100, 1.4 numeric aperture UPlanSApo oil immersion objective was used for image acquisition. Serial *z*-stacks (0.25 μm distance) were acquired before the application of quencher for each dish imaged to indicate the presence of fibrils. Trypan blue solution (1 ml, 1 mM in DBPS) was added dropwise to the dish and mixed by gentle pipetting for a final concentration of 500 μM trypan blue. At least five serial *z*-stacks were acquired for each plate (λ_{ex} = 488, λ_{em} = 525/50 for GFP; λ_{ex} = 561, λ_{em} = 630/75 for trypan blue). *x*-*y* dimensions were defined by live bright field imaging, and *z*-dimensions were defined for each *z*-stack by using trypan blue fluorescence to identify the bottom and top of the culture in each frame. For trypan blue-quenched conditions, fibril fluorescence was not observed prior to image acquisition. Time course experiments utilized separate dishes, which were quenched at the time indicated. No evidence of increased detectable intracellular puncta was observed over the course of imaging quenched cultures (<10 min), probably due to uptake of quencher along with pffs during this time period. Uptake data were quantified using the ImageJ 3D object identification algorithm, using intensity thresholds established from measurements of cellular

autofluorescence of PBS (vehicle)-treated neurons during each experiment. Unless otherwise noted, all E114C-labeled pffs were transduced at 0.5 μg per dish to be consistent with the amount of α-syn added for mSyn-GFP pff transductions, and images were acquired similarly.

Inhibition of mSyn–GFP uptake

To validate the trypan blue quenching approach for the measurement of intracellular fibrils, uptake of mSyn–GFP pffs was inhibited thermally, by heparin treatment, and shown to be largely sonication-dependent. For low-temperature experiments, neurons were briefly chilled to 4 °C in a refrigerator for 10 min prior to transduction as above with a pff suspension pre-equilibrated to 4 °C. Neurons were incubated for 30 min at 4 °C followed by an additional 30-min incubation at 4 °C for experimental dishes or 37 °C for control dishes. All cultures were immediately imaged at room temperature after the timed incubation. For inhibition by heparin, pffs were diluted to sonication concentrations in DPBS containing 200 μM heparin (Sigma-Aldrich) or acetate buffer (vehicle control, 2% (v/v)) and incubated overnight. α-Syn pffs were sonicated and diluted in neuronal medium containing 100 μM heparin or vehicle. Neurons were transduced with pffs (1.5 μg/dish) in the presence of 100 μM heparin or vehicle control as above. For examination of the effects of sonication on α-syn pff uptake, pffs were diluted for delivery to neurons in separate Eppendorf tubes, one of which was subjected to sonication. Otherwise, dilution and pff transduction were performed as above. Neurons were imaged 1 h pTd. All experiments were conducted in duplicate plates on three separate days.

pff treatments for immunocytochemical analysis

Primary neurons growing on a 13-mm German coverglass in 24-well plates were treated as described previously (20, 23). Briefly, pffs were diluted to 100 μM and sonicated as above. pffs were diluted 20× in neuronal medium and added to neuronal cultures. Medium was exchanged every 3–4 days pTd before fixation and staining.

Perturbation of lysosomal activity and integrity by CHQ pulse

Neurons growing on 13-mm German glass coverslips were transduced as above for 3 h in a total volume of 0.5 ml of neuronal medium + α-syn pff suspension or DPBS vehicle. 0.5 ml of a 200 μM solution of CHQ or DPBS vehicle (0.1%, v/v) in neuronal medium was added to each well for a final concentration of 100 μM CHQ. Cultures were incubated for 30 min. Coverslips were physically removed from treatment wells with forceps, dipped three times in separate containers of DBPS wash buffer, and added to wells of a separate plate containing 0.5 ml of a 3:1 mixture of filtered conditioned medium/complete neuronal medium. Cells were incubated for the indicated times prior to fixation and immunocytochemical analysis.

Immunocytochemistry

Neurons were fixed at the indicated times with solutions of 4% (v/v) paraformaldehyde (Electron Microscopy Systems) and 4% (w/v) sucrose (Sigma-Aldrich) in DPBS. Cells were incubated in fixative for 15–20 min and washed three times with DPBS before permeabilization with 0.1% Triton X-100 in DPBS and an additional three washes with DPBS. Cells were blocked for 1 h at room temperature with a solution of 3% BSA (Corning) and 5% FBS (Gibco) in DPBS (immunocytochemistry block buffer). Samples were incubated with primary antibodies for either 2 h at room temperature or overnight at 4 °C. Primary antibodies were washed three times with DPBS before treatment with fluorophore-conjugated secondary antibodies for 1 h at room temperature. Samples were washed twice in DPBS and twice in deionized H_2O. Coverslips were mounted on Fisher glass slides in DAPI-Fluoromount and allowed to cure overnight before imaging.

Automated digital image acquisition and analysis of fixed neurons

Digital images of slide-mounted coverslips were acquired at ×20 magnification using a Lamina (PerkinElmer Life Sciences) slide scanner with a pixel size of 6.5 μm^2 (*i.e.* pixel resolution of 0.325 μm), camera resolution of 2560 × 2160, and a bit depth of 16. HALO digital image software version 1.90 (Indica Labs, Albuquerque, NM) was utilized to develop detection algorithms to quantify α-syn pathology, MAP2 coverage, and nuclei. Objects of interest were identified using intensity thresholding and size restrictions, confirmed with visual inspection across all conditions. Single-sized regions of interest were stamped on all coverslips, with areas of folded or torn cell monolayers excluded manually.

STED imaging of fixed neurons

For STED imaging experiments, neurons were treated with $\alpha S\text{-}C^{Bdp}{}_{114}$ with and without CHQ and fixed as above. Cells were stained with 81A (Covance) followed by goat anti-mouse Alexa Fluor 532 (Thermo Fisher) and mounted using ProLong® Diamond Antifade (Thermo Fisher). Images were acquired on a TCS SP8 gSTED 3X microscope (Leica, Buffalo Grove, IL). Fluorescence excitation was provided by a white-light laser set to 492 nm for BODIPY and 532 nm for Alexa Fluor 532, and depletion lasers used were 594 nm (for BODIPY) and 660 nm (for Alexa Fluor 538). Coverslips were imaged using an HC PL APO ×100/1.40 numeric aperture oil objective, and serial *z*-stacks were acquired in 0.25-μm increments.

Western blot analysis of mSyn–GFP pffs at 5 days pTd

Sequential extraction and Western blot analysis of cellular lysate from primary hippocampal neurons 5 days after pff treatment were conducted as described previously. (23). For detailed information, see the supplemental data.

Immunoelectron microscopy of α-syn seed uptake and intracellular persistence

Immuno-EM was conducted as described previously (23), using anti-BODIPY (Fisher) or Syn 204 antibodies as indicated. Cells for anti-BODIPY treatment were fixed 20 min in 2% paraformaldehyde + 0.05% glutaraldehyde in 0.1 M cacodylate buffer, pH 7.4. All other cultures were fixed for 2 h in periodate/lysine/paraformaldehyde. Cells for nanogold stain were permeabilized for 10 min in 50% ethanol before immunostaining. The nanogold-labeled cells were postfixed for 20 min in 1%

osmium tetroxide in 0.1 M cacodylate buffer, pH 7.4, gold-toned for 5 min in 0.05% gold chloride, postfixed for 20 min in 1% OsO_4 and 1.5% potassium ferrocyanide in 0.05 M cacodylate buffer, and dehydrated and embedded in Epon. Transmission EM images were collected using a Jeol 1010 electron microscope at the University of Pennsylvania Biomedical Imaging Core.

Author contributions—R. J. K. and V. M.-Y. L. conceived and coordinated the study and wrote the paper. E. J. P. conceived and coordinated the production, characterization, and application of the E114C-labeled α-synuclein used in this study. R. J. K. designed, performed, and analyzed the neuronal pff uptake experiments. C. M. H. and T. S. M. designed, performed, and analyzed experiments regarding production and characterization of E114C-labeled α-synuclein species. R. M. S. provided technical assistance, replicated key results, and analyzed data. All authors reviewed the results, edited the manuscript, and approved the final version for submission.

Acknowledgments—We thank Dawn M. Riddle for providing primary neurons, Matthew D. Byrne and Kyle J. McKee for technical assistance, Anna Steiber for the immuno-EM experiments, and Dr. Andrea Stout for helpful discussions regarding confocal microscopy experiments. All confocal images were acquired with instruments from the University of Pennsylvania Cell and Developmental Biology Microscopy Core. Instruments supported by the National Science Foundation (NSF) include the CD spectrometer (NSF Grant DMR05-20020) and the MALDI mass spectrometer (NSF Grant MRI-0820996).

Note added in proof—In supplemental Fig. 2, the human α S-C114 BODIPY MALDI-TOF spectra were inadvertently duplicated to represent the mouse α S-C114 BODIPY MALDI–TOF spectra in the version of this article that was published as a Paper in Press on June 13, 2017. This error has now been corrected and does not affect the results or conclusions of this work.

References

1. Jucker, M., and Walker, L. C. (2013) Self-propagation of pathogenic protein aggregates in neurodegenerative diseases. *Nature* **501,** 45–51
2. Guo, J. L., and Lee, V. M. (2014) Cell-to-cell transmission of pathogenic proteins in neurodegenerative diseases. *Nat. Med.* **20,** 130–138
3. Spillantini, M. G., Crowther, R. A., Jakes, R., Hasegawa, M., and Goedert, M. (1998) α-Synuclein in filamentous inclusions of Lewy bodies from Parkinson's disease and dementia with Lewy bodies. *Proc. Natl. Acad. Sci. U.S.A.* **95,** 6469–6473
4. Goedert, M., and Spillantini, M. G. (1998) Lewy body diseases and multiple system atrophy as α-synucleinopathies. *Mol. Psychiatry* **3,** 462–465
5. Hansen, C., Angot, E., Bergström, A. L., Steiner, J. A., Pieri, L., Paul, G., Outeiro, T. F., Melki, R., Kallunki, P., Fog, K., Li, J. Y., and Brundin, P. (2011) α-Synuclein propagates from mouse brain to grafted dopaminergic neurons and seeds aggregation in cultured human cells. *J. Clin. Invest.* **121,** 715–725
6. Luk, K. C., Kehm, V., Carroll, J., Zhang, B., O'Brien, P., Trojanowski, J. Q., and Lee, V. M. (2012) Pathological α-synuclein transmission initiates Parkinson-like neurodegeneration in nontransgenic mice. *Science* **338,** 949–953
7. Luk, K. C., Kehm, V. M., Zhang, B., O'Brien, P., Trojanowski, J. Q., and Lee, V. M. (2012) Intracerebral inoculation of pathological α-synuclein initiates a rapidly progressive neurodegenerative α-synucleinopathy in mice. *J. Exp. Med.* **209,** 975–986
8. Paumier, K. L., Luk, K. C., Manfredsson, F. P., Kanaan, N. M., Lipton, J. W., Collier, T. J., Steece-Collier, K., Kemp, C. J., Celano, S., Schulz, E., Sandoval, I. M., Fleming, S., Dirr, E., Polinski, N. K., Trojanowski, J. Q., *et al.* (2015) Intrastriatal injection of pre-formed mouse α-synuclein fibrils into rats triggers α-synuclein pathology and bilateral nigrostriatal degeneration. *Neurobiol. Dis.* **82,** 185–199
9. Peelaerts, W., Bousset, L., Van der Perren, A., Moskalyuk, A., Pulizzi, R., Giugliano, M., Van den Haute, C., Melki, R., and Baekelandt, V. (2015) α-Synuclein strains cause distinct synucleinopathies after local and systemic administration. *Nature* **522,** 340–344
10. Recasens, A., Dehay, B., Bové, J., Carballo-Carbajal, I., Dovero, S., Pérez-Villalba, A., Fernagut, P. O., Blesa, J., Parent, A., Perier, C., Fariñas, I., Obeso, J. A., Bezard, E., and Vila, M. (2014) Lewy body extracts from Parkinson disease brains trigger α-synuclein pathology and neurodegeneration in mice and monkeys. *Ann. Neurol.* **75,** 351–362
11. Holmes, B. B., DeVos, S. L., Kfoury, N., Li, M., Jacks, R., Yanamandra, K., Ouidja, M. O., Brodsky, F. M., Marasa, J., Bagchi, D. P., Kotzbauer, P. T., Miller, T. M., Papy-Garcia, D., and Diamond, M. I. (2013) Heparan sulfate proteoglycans mediate internalization and propagation of specific proteopathic seeds. *Proc. Natl. Acad. Sci. U.S.A.* **110,** E3138–E3147
12. Mirbaha, H., Holmes, B. B., Sanders, D. W., Bieschke, J., and Diamond, M. I. (2015) Tau trimers are the minimal propagation unit spontaneously internalized to seed intracellular aggregation. *J. Biol. Chem.* **290,** 14893–14903
13. Wu, J. W., Herman, M., Liu, L., Simoes, S., Acker, C. M., Figueroa, H., Steinberg, J. I., Margittai, M., Kayed, R., Zurzolo, C., Di Paolo, G., and Duff, K. E. (2013) Small misfolded Tau species are internalized via bulk endocytosis and anterogradely and retrogradely transported in neurons. *J. Biol. Chem.* **288,** 1856–1870
14. Freundt, E. C., Maynard, N., Clancy, E. K., Roy, S., Bousset, L., Sourigues, Y., Covert, M., Melki, R., Kirkegaard, K., and Brahic, M. (2012) Neuron-to-neuron transmission of α-synuclein fibrils through axonal transport. *Ann. Neurol.* **72,** 517–524
15. Brahic, M., Bousset, L., Bieri, G., Melki, R., and Gitler, A. D. (2016) Axonal transport and secretion of fibrillar forms of α-synuclein, Aβ42 peptide and HTTExon 1. *Acta Neuropathol.* **131,** 539–548
16. Loike, J. D., and Silverstein, S. C. (1983) A fluorescence quenching technique using trypan blue to differentiate between attached and ingested glutaraldehyde-fixed red blood cells in phagocytosing murine macrophages. *J. Immunol. Methods* **57,** 373–379
17. Hed, J., Hallden, G., Johansson, S. G., and Larsson, P. (1987) The use of fluorescence quenching in flow cytofluorometry to measure the attachment and ingestion phases in phagocytosis in peripheral blood without prior cell separation. *J. Immunol. Methods* **101,** 119–125
18. Wan, C. P., Park, C. S., and Lau, B. H. (1993) A rapid and simple microfluorometric phagocytosis assay. *J. Immunol. Methods* **162,** 1–7
19. Stopa, B., Piekarska, B., Konieczny, L., Rybarska, J., Spólnik, P., Zemanek, G., Roterman, I., and Król, M. (2003) The structure and protein binding of amyloid-specific dye reagents. *Acta Biochim. Polonica* **50,** 1213–1227
20. Volpicelli-Daley, L. A., Luk, K. C., and Lee, V. M. (2014) Addition of exogenous α-synuclein preformed fibrils to primary neuronal cultures to seed recruitment of endogenous α-synuclein to Lewy body and Lewy neurite-like aggregates. *Nat. Protoc.* **9,** 2135–2146
21. Hansen, C., Björklund, T., Petit, G. H., Lundblad, M., Murmu, R. P., Brundin, P., and Li, J. Y. (2013) A novel α-synuclein-GFP mouse model displays progressive motor impairment, olfactory dysfunction and accumulation of α-synuclein-GFP. *Neurobiol. Dis.* **56,** 145–155
22. Osterberg, V. R., Spinelli, K. J., Weston, L. J., Luk, K. C., Woltjer, R. L., and Unni, V. K. (2015) Progressive aggregation of α-synuclein and selective degeneration of Lewy inclusion-bearing neurons in a mouse model of parkinsonism. *Cell Rep.* **10,** 1252–1260
23. Volpicelli-Daley, L. A., Luk, K. C., Patel, T. P., Tanik, S. A., Riddle, D. M., Stieber, A., Meaney, D. F., Trojanowski, J. Q., and Lee, V. M. (2011) Exogenous α-synuclein fibrils induce Lewy body pathology leading to synaptic dysfunction and neuron death. *Neuron* **72,** 57–71
24. Kneen, M., Farinas, J., Li, Y., and Verkman, A. S. (1998) Green fluorescent protein as a noninvasive intracellular pH indicator. *Biophys. J.* **74,** 1591–1599
25. Bae, E. J., Yang, N. Y., Lee, C., Kim, S., Lee, H. J., and Lee, S. J. (2015) Haploinsufficiency of cathepsin D leads to lysosomal dysfunction and pro-

motes cell-to-cell transmission of α-synuclein aggregates. *Cell Death Dis.* **6,** e1901
26. Karolin, J., Johansson, L. B. A., Strandberg, L., and Ny, T. (1994) Fluorescence and absorption spectroscopic properties of dipyrrometheneboron difluoride (Bodipy) derivatives in liquids, lipid-membranes, and proteins. *J. Am. Chem. Soc.* **116,** 7801–7806
27. Loudet, A., and Burgess, K. (2007) BODIPY dyes and their derivatives: syntheses and spectroscopic properties. *Chem. Rev.* **107,** 4891–4932
28. Haney, C. M., Wissner, R. F., Warner, J. B., Wang, Y. J., Ferrie, J. J., Covell, D. J., Karpowicz R. J., Lee, V. M., and Petersson, E. J. (2016) Comparison of strategies for non-perturbing labeling of α-synuclein to study amyloidogenesis. *Org. Biomol. Chem.* **14,** 1584–1592
29. Miksa, M., Komura, H., Wu, R., Shah, K. G., and Wang, P. (2009) A novel method to determine the engulfment of apoptotic cells by macrophages using pHrodo succinimidyl ester. *J. Immunol. Methods* **342,** 71–77
30. Tran, H. T., Chung, C. H., Iba, M., Zhang, B., Trojanowski, J. Q., Luk, K. C., and Lee, V. M. (2014) α-Synuclein immunotherapy blocks uptake and templated propagation of misfolded α-synuclein and neurodegeneration. *Cell Rep.* **7,** 2054–2065
31. Luthman, H., and Magnusson, G. (1983) High efficiency polyoma DNA transfection of chloroquine treated cells. *Nucleic Acids Res.* **11,** 1295–1308
32. Erbacher, P., Roche, A. C., Monsigny, M., and Midoux, P. (1996) Putative role of chloroquine in gene transfer into a human hepatoma cell line by DNA/lactosylated polylysine complexes. *Exp. Cell Res.* **225,** 186–194
33. Schenborn, E. T., and Goiffon, V. (2000) DEAE-dextran transfection of mammalian cultured cells. *Methods Mol. Biol.* **130,** 147–153
34. Ciftci, K., and Levy, R. J. (2001) Enhanced plasmid DNA transfection with lysosomotropic agents in cultured fibroblasts. *Int. J. Pharm.* **218,** 81–92
35. Sacino, A. N., Brooks, M. M., Chakrabarty, P., Saha, K., Khoshbouei, H., Golde, T. E., and Giasson, B. I. (2017) Proteolysis of α-synuclein fibrils in the lysosomal pathway limits induction of inclusion pathology. *J. Neurochem.* **140,** 662–678
36. Wibo, M., and Poole, B. (1974) Protein degradation in cultured cells. II. The uptake of chloroquine by rat fibroblasts and the inhibition of cellular protein degradation and cathepsin B1. *J. Cell Biol.* **63,** 430–440
37. Yoon, Y. H., Cho, K. S., Hwang, J. J., Lee, S. J., Choi, J. A., and Koh, J. Y. (2010) Induction of lysosomal dilatation, arrested autophagy, and cell death by chloroquine in cultured ARPE-19 cells. *Invest. Ophthalmol. Vis. Sci.* **51,** 6030–6037
38. Michihara, A., Toda, K., Kubo, T., Fujiwara, Y., Akasaki, K., and Tsuji, H. (2005) Disruptive effect of chloroquine on lysosomes in cultured rat hepatocytes. *Biol. Pharm. Bull.* **28,** 947–951
39. Fröhlich, E., Meindl, C., Roblegg, E., Ebner, B., Absenger, M., and Pieber, T. R. (2012) Action of polystyrene nanoparticles of different sizes on lysosomal function and integrity. *Part. Fibre Toxicol.* **9,** 26
40. Apetri, M. M., Harkes, R., Subramaniam, V., Canters, G. W., Schmidt, T., and Aartsma, T. J. (2016) Direct observation of α-synuclein amyloid aggregates in endocytic vesicles of neuroblastoma cells. *PLoS One* **11,** e0153020
41. Freeman, D., Cedillos, R., Choyke, S., Lukic, Z., McGuire, K., Marvin, S., Burrage, A. M., Sudholt, S., Rana, A., O'Connor, C., Wiethoff, C. M., and Campbell, E. M. (2013) α-Synuclein induces lysosomal rupture and cathepsin dependent reactive oxygen species following endocytosis. *PLoS One* **8,** e62143
42. Flavin, W. P., Bousset, L., Green, Z. C., Chu, Y., Skarpathiotis, S., Chaney, M. J., Kordower, J. H., Melki, R., and Campbell, E. M. (2017) Endocytic vesicle rupture is a conserved mechanism of cellular invasion by amyloid proteins. *Acta Neuropathol.* 10.1007/s00401-017-1722-x
43. Volles, M. J., Lee, S. J., Rochet, J. C., Shtilerman, M. D., Ding, T. T., Kessler, J. C., and Lansbury, P. T., Jr. (2001) Vesicle permeabilization by protofibrillar α-synuclein: implications for the pathogenesis and treatment of Parkinson's disease. *Biochemistry* **40,** 7812–7819
44. Pacheco, C., Aguayo, L. G., and Opazo, C. (2012) An extracellular mechanism that can explain the neurotoxic effects of α-synuclein aggregates in the brain. *Front. Physiol.* **3,** 297
45. Flach, K., Hilbrich, I., Schiffmann, A., Gärtner, U., Krüger, M., Leonhardt, M., Waschipky, H., Wick, L., Arendt, T., and Holzer, M. (2012) Tau oligomers impair artificial membrane integrity and cellular viability. *J. Biol. Chem.* **287,** 43223–43233
46. Samuel, F., Flavin, W. P., Iqbal, S., Pacelli, C., Sri Renganathan, S. D., Trudeau, L. E., Campbell, E. M., Fraser, P. E., and Tandon, A. (2016) Effects of serine 129 phosphorylation on α-synuclein aggregation, membrane association, and internalization. *J. Biol. Chem.* **291,** 4374–4385
47. Dehay, B., Martinez-Vicente, M., Ramirez, A., Perier, C., Klein, C., Vila, M., and Bezard, E. (2012) Lysosomal dysfunction in Parkinson disease: ATP13A2 gets into the groove. *Autophagy* **8,** 1389–1391
48. Ramirez, A., Heimbach, A., Gründemann, J., Stiller, B., Hampshire, D., Cid, L. P., Goebel, I., Mubaidin, A. F., Wriekat, A. L., Roeper, J., Al-Din, A., Hillmer, A. M., Karsak, M., Liss, B., Woods, C. G., *et al.* (2006) Hereditary parkinsonism with dementia is caused by mutations in ATP13A2, encoding a lysosomal type 5 P-type ATPase. *Nat. Genet.* **38,** 1184–1191
49. Rosenbloom, B., Balwani, M., Bronstein, J. M., Kolodny, E., Sathe, S., Gwosdow, A. R., Taylor, J. S., Cole, J. A., Zimran, A., and Weinreb, N. J. (2011) The incidence of Parkinsonism in patients with type 1 Gaucher disease: data from the ICGG Gaucher Registry. *Blood Cells Mol. Dis.* **46,** 95–102
50. Goker-Alpan, O., Stubblefield, B. K., Giasson, B. I., and Sidransky, E. (2010) Glucocerebrosidase is present in α-synuclein inclusions in Lewy body disorders. *Acta Neuropathol.* **120,** 641–649
51. Vilariño-Güell, C., Wider, C., Ross, O. A., Dachsel, J. C., Kachergus, J. M., Lincoln, S. J., Soto-Ortolaza, A. I., Cobb, S. A., Wilhoite, G. J., Bacon, J. A., Behrouz, B., Melrose, H. L., Hentati, E., Puschmann, A., Evans, D. M., *et al.* (2011) VPS35 mutations in Parkinson disease. *Am. J. Hum. Genet.* **89,** 162–167
52. Zimprich, A., Benet-Pagès, A., Struhal, W., Graf, E., Eck, S. H., Offman, M. N., Haubenberger, D., Spielberger, S., Schulte, E. C., Lichtner, P., Rossle, S. C., Klopp, N., Wolf, E., Seppi, K., Pirker, W., *et al.* (2011) A mutation in VPS35, encoding a subunit of the retromer complex, causes late-onset Parkinson disease. *Am. J. Hum. Genet.* **89,** 168–175
53. Tang, F. L., Erion, J. R., Tian, Y., Liu, W., Yin, D. M., Ye, J., Tang, B., Mei, L., and Xiong, W. C. (2015) VPS35 in dopamine neurons is required for endosome-to-Golgi retrieval of Lamp2a, a receptor of chaperone-mediated autophagy that is critical for α-synuclein degradation and prevention of pathogenesis of Parkinson's disease. *J. Neurosci.* **35,** 10613–10628
54. Qiao, L., Hamamichi, S., Caldwell, K. A., Caldwell, G. A., Yacoubian, T. A., Wilson, S., Xie, Z. L., Speake, L. D., Parks, R., Crabtree, D., Liang, Q., Crimmins, S., Schneider, L., Uchiyama, Y., Iwatsubo, T., *et al.* (2008) Lysosomal enzyme cathepsin D protects against α-synuclein aggregation and toxicity. *Mol. Brain* **1,** 17
55. Cullen, V., Lindfors, M., Ng, J., Paetau, A., Swinton, E., Kolodziej, P., Boston, H., Saftig, P., Woulfe, J., Feany, M. B., Myllykangas, L., Schlossmacher, M. G., and Tyynelä, J. (2009) Cathepsin D expression level affects α-synuclein processing, aggregation, and toxicity *in vivo*. *Mol. Brain* **2,** 5
56. Bendor, J. T., Logan, T. P., and Edwards, R. H. (2013) The function of α-synuclein. *Neuron* **79,** 1044–1066
57. Bourdenx, M., Bezard, E., and Dehay, B. (2014) Lysosomes and α-synuclein form a dangerous duet leading to neuronal cell death. *Front. Neuroanat.* **8,** 83
58. Mao, X., et al. (2016) Pathological α-synuclein transmission initiated by binding lymphocyte-activation gene 3. *Science* 10.1126/science.aah3374
59. Abounit, S., Bousset, L., Loria, F., Zhu, S., de Chaumont, F., Pieri, L., Olivo-Marin, J. C., Melki, R., and Zurzolo, C. (2016) Tunneling nanotubes spread fibrillar α-synuclein by intercellular trafficking of lysosomes. *EMBO J.* **35,** 2120–2138
60. Bieri, G., Gitler, A. D., and Brahic, M. (2017) Internalization, axonal transport and release of fibrillar forms of α-synuclein. *Neurobiol. Dis.* 10.1016/j.nbd.2017.03.007
61. Giasson, B. I., Murray, I. V., Trojanowski, J. Q., and Lee, V. M. (2001) A hydrophobic stretch of 12 amino acid residues in the middle of α-synuclein is essential for filament assembly. *J. Biol. Chem.* **276,** 2380–2386